Available online at www.sciencedirect.com
SCIENCE DIRECT®
Bioorganic & Medicinal Chemistry 13 (2005) 4835–4841
Bioorganic & Medicinal Chemistry

RO4383596, an orally active KDR, FGFR, and PDGFR inhibitor: Synthesis and biological evaluation

Lee A. McDermott,*,† Mary Simcox, Brian Higgins, Tom Nevins, Kenneth Kolinsky, Melissa Smith, Hong Yang, Jia K. Li, Yingsi Chen, June Ke, Navita Mallalieu, Tom Egan, Stan Kolis, Aruna Railkar, Louise Gerber and Kin-Chun Luk

Hoffmann-La Roche Inc., 340 Kingsland Str., Nutley, NJ 07110, USA

Received 21 April 2005; accepted 6 May 2005
Available online 13 June 2005

Abstract—(±)-1-(*anti*-3-Hydroxy-cyclopentyl)-3-(4-methoxy-phenyl)-7-phenylamino-3,4-dihydro-1*H*-pyrimido[4,5-*d*]pyrimidin-2-one (RO4383596) is a potent and selective inhibitor of the pro-angiogenic receptor tyrosine kinases KDR, FGFR, and PDGFR. This agent has an excellent pharmacokinetic profile and is highly efficacious in rodent models of angiogenesis upon oral administration.

1. Introduction

The growth and metastasis of a great number of malignant tumors is highly dependent on their ability to induce the formation of a vasculature that can supply them with blood and nutrients (angiogenesis).[1,2] Since this realization, in the 1970s,[3] there has been an intense pursuit for agents that can inhibit this process for the treatment of cancer. As of this writing, there were over 150 clinical trials, registered with the US FDA, evaluating drugs that can interrupt cancer-induced angiogenesis via various mechanisms.[4] Particular emphasis has been placed on the development of anti-angiogenic, orally administered, small molecules that act through the inhibition of receptor tyrosine kinases (RTKs) directly involved in pro-angiogenic signaling cascades.[5,6] Focus was initially placed on the synthesis of molecules that were selective for individual pro-angiogenic RTKs. However, emerging preclinical data appear to suggest that the targeting of multiple pro-angiogenic RTKs may confer better therapeutic outcomes than the selective targeting of only one such kinase.[7] In this paper, we describe the synthesis and biological evaluation of RO4383596, an orally bioavailable small molecule ATP-competitive inhibitor of three key angiogenesis-involved RTKs, the KDR, FGFR, and PDGFR.

2. Chemistry

RO4383596 (**6**, Scheme 1) is a racemic pyrimidopyrimidone and a member of a series that we reported on recently.[8]

Its synthesis started with the commercially available pyrimidine **1**. This pyrimidine was first reacted with

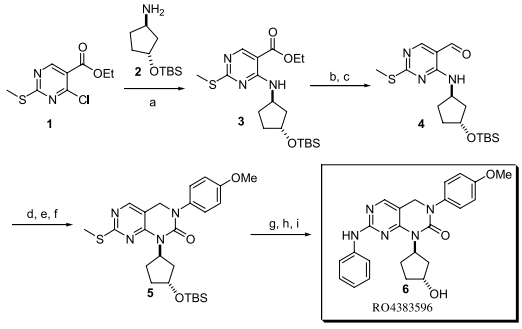

Scheme 1. Reagents and conditions: (a) dioxane, 1 equiv of **2**, 2 equiv Et_3N reflux; (b) THF, 3.2 equiv $LiAlH_4$, rt; (c) CH_2Cl_2, 10 equiv MnO_2 (62% yield for three steps); (d) toluene, 1 equiv *p*-methoxy-aniline, cat. TsOH, reflux; (e) THF, 3 equiv $LiAlH_4$, rt; (f) CH_2Cl_2, 3 equiv Et_3N, 1.1 equiv $COCl_2$ 20% in toluene (57% yield for three steps); (g) THF, 2.1 equiv of *m*CPBA, rt; (h) aniline, 100–110 °C; (i) 25% TFA in CH_2Cl_2, 0 °C (73% yield for three steps).

Keywords: KDR inhibitor; VEGFR inhibitor; PDGFR inhibitor; FGFR inhibitor; Pyrimidopyrimidone; RO4383596.
* Corresponding author. Tel.: +1 973 235 6307; fax: +1 973 235 2448; e-mail: lee.mcdermott@roche.com
† f/k/a Apostolos Dermatakis.

0968-0896/$ - see front matter © 2005 Elsevier Ltd. All rights reserved.
doi:10.1016/j.bmc.2005.05.012

the known racemic TBS-protected aminocyclopentanol **2**[9] in refluxing dioxane to afford ester **3**. After a reduction with $LiAlH_4$ and a subsequent oxidation with MnO_2, ester **3** was transformed to the corresponding methylthio-aminopyrimidine aldehyde **4**. This aldehyde intermediate was then condensed with *p*-anisidine to yield the corresponding *p*-anisidine-imine that, in turn, after a reduction with $LiAlH_4$ and a cyclization with phosgene was converted to methylthio-pyrimidopyrimidone **5**. From pyrimidone **5**, RO4383596 was accessed in three steps. First, **5** was treated with *m*CPBA. This treatment was then followed by heating at 90 °C in neat aniline to afford the respective O-TBS-protected RO4383596 intermediate. The deprotection of that compound to RO4383596 was effected by a treatment with 25% TFA in CH_2Cl_2.

3. Biological results

3.1. Kinase selectivity and cellular potency

RO4383596 is a potent and selective inhibitor of KDR, FGFR, and PDGFR.[10] In a panel of 12 kinases, RO4383596 potently inhibited those three kinases with low double digit nanomolar potency. It was between 10- and 3000-fold less potent against the other kinases of that panel (Table 1).

In cellular assays, RO4383596 potently and selectively inhibited the proliferation of endothelial cells that was driven by either VEGF or bFGF. Western blot analysis of VEGF-stimulated human umbilical cord endothelial cells (HUVECs) treated with RO4383596 showed a dose-dependent inhibition of KDR autophosphorylation along with dose-dependent inhibition of phosphorylation/activation of the downstream effector kinases Erk1/2 and AKT (Fig. 1). Also, as shown in Table 2, RO4383596 potently inhibited endothelial cell proliferation driven by either bFGF or VEGF but did not inhibit to any appreciable extent the proliferation of RKO or MDA-MB-435 cancer cells. RKO and MDA-MB-435 cancer cell proliferation, unlike endothelial cell proliferation, is not dependent on the signaling cascades that KDR, FGFR or PDGFR are involved in.

Table 1. Kinase selectivity profile of RO4383596

Kinase	IC_{50} (nM)[a]
KDR	44
FGFR	29
PDGFR	33
EGFR	310
Fyn	322
EphB3	1,090
Erk2	3,040
SGK	>125,000
AKT	>125,000
PKCα	>125,000
PKCδ	>125,000
CDK1	>125,000

[a] IC_{50} values determined by a single experiment run in duplicate.

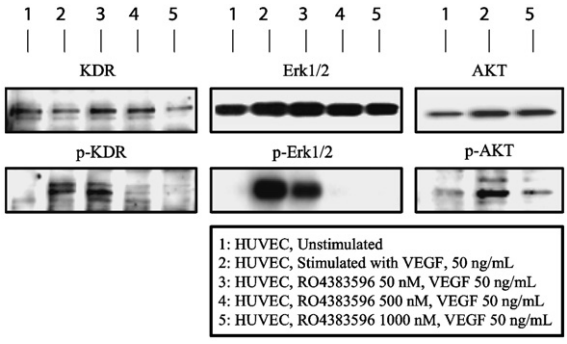

Figure 1. Inhibition of KDR autophosphorylation and inhibition of phosphorylation/activation of the downstream effector kinases Erk1/2 and AKT in RO4383596-treated human umbilical vein endothelial cells (HUVECs).

Table 2. Inhibition of cellular proliferation by RO4383596

Cell line	IC_{50} (nM)[a]
HUVEC[b]	68
HUVEC[c]	150
RKO	2300
MDA-MB-435	4200

[a] IC_{50} values determined by a single experiment run in duplicate.
[b] Proliferation promoted by VEGF.
[c] Proliferation promoted by bFGF.

The inactivity of RO4383596 against the RKO and MDA-MB-435 cells along with the inhibition of activation of downstream effector kinases in RO4383596-treated endothelial cells suggests that the antiproliferative effects seen with the HUVEC cell line are mechanism-based and not due to RO4383596 acting as a cytotoxic agent.

3.2. Rodent pharmacokinetics

The potency and selectivity in vitro of RO4383596 was accompanied by a very good overall pharmacokinetic profile.

Testing in athymic nude mice and Wistar rats revealed that, in both species, RO4383596 has good clearance parameters (Table 3). That was coupled with a high oral bioavailability and plasma exposure (Table 4). In addition, as shown in Table 5, this agent exhibits a linear pharmacokinetic profile. Plasma analysis of C57/BL6 mice treated orally twice a day for 5 days with 25, 50 and 100 mg/kg of RO4383596 revealed that there was a dose proportional increase in the observed AUC between these three individual doses.[11]

Table 3. Mean pharmacokinetic parameters after iv administration of RO4383596 in rodents

Species	Cl (mL/min/kg)	AUC (ng h/mL)	V_{dss} (L/kg)	$t_{1/2}$ (h)
Nude mice[a]	15.1	11,058	1.9	3
Wistar rats[b]	23.1	4,014	5.3	6

[a] Single dose, 10 mg/kg.
[b] Single dose, 5 mg/kg.

Table 4. Mean pharmacokinetic parameters after a single 50 mg/kg po administration of RO4383596 in rodents

Species	C_{max} (ng/mL)	AUC (ng h/mL)	T_{max} (h)	F (%)
Nude mice	16,462	51,278	0.25	93
Wistar rats	7,180	26,476	5.3	65

Table 5. Mean pharmacokinetic parameters after twice a day for 5 days po administration of RO4383596 in C57/BL6 female mice

PK parameter	Dose (mg/kg)		
	25	50	100
AUC (ng h/mL)	29,980	75,519	150,275
AUC/dose (ng h/mL/mg/kg)	1,199	1,510	1,458
C_{max} (ng/mL)	12,000	28,4000	47,700
T_{max} (h)	0.5	0.5	0.5

3.3. In vivo efficacy

The ability of RO4383596 to inhibit angiogenesis in vivo was evaluated in a mouse corneal pocket assay.[12]

VEGF- or bFGF-impregnated pellets were implanted in the corneas of C57/BL6 mice. This implantation was followed by a twice a day oral administration of RO4383596 at three separate doses of 25, 50 and 100 mg/kg. Mice that had corneal angiogenesis induced by VEGF were treated with RO4383596 for 7 days. Mice that had corneal neovascularization induced by bFGF were treated with RO4383596 for 5 days. At the end of the treatment periods the area of angiogenesis in the eyes of mice was quantitated.

In the VEGF-induced model of neovascularization, oral administration of RO4383596 at 25 mg/kg twice a day led to an 81% inhibition of corneal angiogenesis while at 100 mg/kg that inhibition was essentially complete (Fig. 2).

The results with the cohort of mice that had corneal angiogenesis induced by bFGF were equally good (Fig. 3).

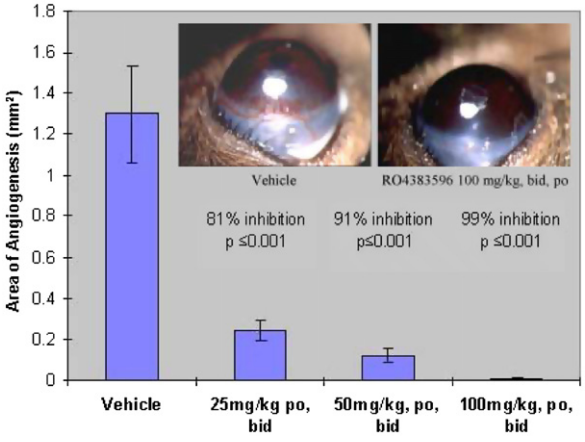

Figure 2. In vivo inhibition of VEGF-induced angiogenesis by RO4383596.

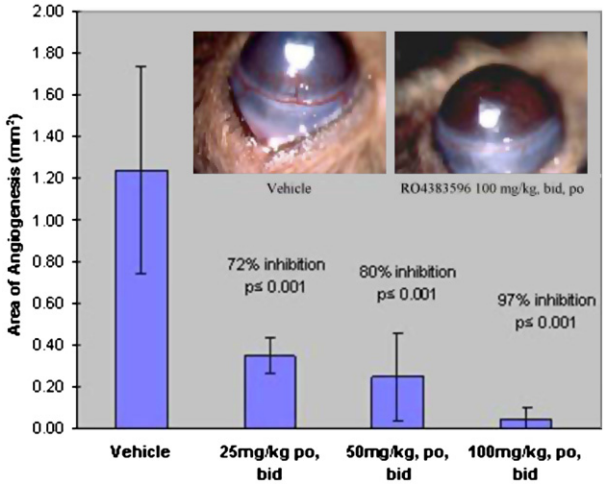

Figure 3. In vivo inhibition of bFGF-induced angiogenesis by RO4383596.

In that model, twice a day oral administration of RO4383596 at 25 mg/kg led to a 72% inhibition of corneal angiogenesis while at 100 mg/kg the inhibition was at 97% relative to that of formulation vehicle treated animals (2% Klucel LF, 0.1% Tween 80 in H_2O).

4. Conclusion

In conclusion, RO4383596 is a pyrimidopyrimidone inhibitor of key receptor tyrosine kinases involved in tumor angiogenesis, namely KDR, FGFR, and PDGFR. In rodents, this agent had high plasma exposure and bioavailability upon oral administration. In vivo it was efficacious at doses as low as 25 mg/kg.

5. Experimental

High resolution mass spectra under EI conditions were obtained with a VG AutoSpec Magnetic Sector spectrometer. Under ES conditions, mass spectra were obtained with a Bruker FTMS (4.7 T) spectrometer while under FAB conditions mass spectra were obtained with a VG 70E Magnetic Sector spectrometer. All high resolution mass spectra were obtained at resolution of 10,000 at 5% valley. ^{1}H NMR spectra were taken with a 300 MHz Varian Mercury or a 400 MHz Varian Unity Spectrometer. Infrared spectra were taken with a Perkin-Elmer Custom GX diffuse reflectance Fourier transform (DRIFTS) spectrometer using KBr or $CHCl_3$ and the spectra were ratioed against a blank spectrum of KBr or $CHCl_3$, respectively. Thin layer chromatography (TLC) was performed on pre-coated silica gel 60 F-254 glass supported plates 0.25 mm thick. Column chromato graphy was performed with silica gel 60 (230–400 mesh). Anhydrous solvents were obtained commercially and were used without further drying. Compounds used in in vivo experiments were analytically pure as judged by HPLC.

5.1. (±)-4-[*anti*-3-(*tert*-Butyl-dimethyl-silanyloxy)-cyclopentylamino]-2-methylsulfanyl-pyrimidine-5-carboxylic acid ethyl ester (3)

A solution of ethyl-4-chloro-2-(methylthio)pyrimidine-5-carboxylate (900 mg, 3.87 mmol) in dioxane (50 mL) was treated with aminocyclopentanol **2**[9] (840 mg, 3.87 mmol) and Et_3N (1.10 mL, 7.74 mmol). The solution was heated at reflux for 30 min and then partitioned between EtOAc and H_2O. The organic layer was dried over Na_2SO_4, filtered and concentrated. The residue was chromatographed on a silica gel column with a 0–20% EtOAc in hexanes gradient to afford **3** as a colorless viscous oil (1.5 g, 94%). IR ($CHCl_3$) 3347, 2957, 2930, 2857, 1681, 1574, 1480, 1430, 1384, 1256, 1160 cm^{-1}. ^1H NMR (300 MHz, $CDCl_3$) δ 0.01 (s, 6H), 0.83 (s, 9H), 1.32 (t, 3H, J = 7.2 Hz), 1.39–1.64 (br m, 3H), 1.94 (m, 1H); 2.08 (m, 1H); 2.26 (apparent sextet, 1H, J = 7.2 Hz), 2.48 (s, 3H), 4.25 (q, 2H, J = 7.2 Hz), 4.32 (m, 1H), 4.67 (apparent sextet, 1H, J = 7.5 Hz), 8.18 (d, 1H, J = 5.1 Hz), 8.55 (s, 1H). HRMS (ES+) for $C_{19}H_{33}N_3O_3SSi$ ($M+H^+$): Calcd 412.2085. Found 412.2088.

5.2. (±)-4-[*anti*-3-(*tert*-Butyl-dimethyl-silanyloxy)-cyclopentylamino]-2-methylsulfanyl-pyrimidine-5-carbaldehyde (4)

A solution of **3** (1.5 g, 3.64 mmol) in THF (80 mL) was treated at 0 °C with solid $LiAlH_4$ (440 mg, 11.61 mmol, added in portions). The reaction mixture was allowed to slowly warm to room temperature and after stirring overnight the reaction mixture was poured slowly into a vigorously stirred biphasic mixture of EtOAc and aqueous saturated Roshell's salt solution. The organic layer was collected, dried over Na_2SO_4, filtered and concentrated to the corresponding benzyl alcohol that was isolated as an off-white solid. ^1H NMR (300 MHz, $CDCl_3$) δ 0.01 (s, 6H), 0.83 (s, 9H), 1.38 (m, 1H), 1.61 (m, 2H), 1.95 (m, 1H); 2.10 (m, 1H), 2.27 (m, 1H), 2.43 (s, 3H), 4.33 (m, 1H), 4.43 (s, 2H), 4.62 (apparent sextet, 1H, J = 7.3 Hz), 5.87 (d, 6.6 Hz), 7.56 (s, 1H). This intermediate was then dissolved in CH_2Cl_2 (80 mL). The resulting solution was treated with MnO_2 (3.36 g, 38.70 mmol) and after stirring overnight was filtered. The solids were washed with approximately 30 mL of THF. The combined organic layer was concentrated and the residue was chromatographed on a silica gel column with a 0–50% Et_2O in hexanes gradient to afford aldehyde **4** as a viscous colorless oil (888 mg, 66%). IR ($CHCl_3$) 3316, 2957, 2931, 2857, 1663, 1584, 1374, 1255 cm^{-1}. ^1H NMR (300 MHz, $CDCl_3$) δ 0.01 (s, 6H), 0.84 (s, 9H), 1.47 (m, 1H), 1.63 (m, 2H), 1.96 (m, 1H), 2.10 (m, 1H), 2.30 (m, 1H), 2.51 (s, 3H), 4.34 (m, 1H), 4.74 (apparent sextet, 1H, J = 7.5 Hz), 8.25 (s, 1H), 8.60 (m, 1H), 9.63 (s, 1H). HRMS (ES+) for $C_{17}H_{29}N_3O_2SSi$ ($M+H^+$): Calcd 368.1823. Found 368.1826.

5.3. (±)-1-[*anti*-3-(*tert*-Butyl-dimethyl-silanyloxy)-cyclopentyl]-3-(4-methoxy-phenyl)-7-methylsulfanyl-3,4-dihydro-1*H*-pyrimido[4,5-*d*]pyrimidin-2-one (5)

A solution of pyrimidine aldehyde **4** (700 mg, 1.90 mmol) in benzene was treated with *p*-anisidine (230 mg, 1.90 mmol) and a catalytic amount of TsOH (50 mg). The mixture was refluxed in a Dean–Stark apparatus for 6 h then cooled and partitioned between EtOAc and aqueous saturated K_2CO_3. The organic layer was collected, dried over Na_2SO_4, filtered and concentrated to afford the corresponding imine intermediate. ^1H NMR (300 MHz, $CDCl_3$) δ 0.01 (s, 6H), 0.84 (s, 9H), 1.45–1.76 (m, 3H), 1.96 (m, 1H), 2.12 (m, 1H), 2.30 (m, 1H), 2.51 (s, 3H), 3.78 (s, 3H), 4.36 (m, 1H), 4.69 (apparent sextet, 1H, J = 6.9 Hz), 6.87 (d, 2H, J = 8.7 Hz), 7.11 (d, 2H, J = 8.7 Hz), 8.05 (s, 1H), 8.32 (s, 1H), 9.87 (d, 1H, J = 6.3 Hz). Without delay this imine intermediate was dissolved in anhydrous THF (60 mL) and to this solution was added, in portions at 0 °C, $LiAlH_4$ (216 mg, 5.70 mmol). The mixture was allowed to slowly warm up to room temperature and after overnight stirring it was poured slowly into a vigorously stirred biphasic mixture of EtOAc and aqueous saturated solution of Roshell's salt. The organic layer was collected, dried over Na_2SO_4, filtered, concentrated and the residue was chromatographed on a normal phase HPLC with a 0–50% Et_2O in hexanes gradient to afford the corresponding benzyl amine intermediate as a foamy off-white solid (574 mg, 64% in two steps). ^1H NMR (300 MHz, $CDCl_3$) δ 0.03 (s, 6H), 0.84 (s, 9H), 1.33 (m, 1H), 1.53 (m, 2H), 1.88 (m, 1H), 2.06 (m, 1H), 2.24 (m, 1H), 2.49 (s, 3H), 3.74 (s, 3H), 3.99 (s, 2H), 4.27 (m, 1H), 4.60 (apparent sextet, 1H, J = 7.2 Hz), 6.10 (br d, 1H, J = 5.7 Hz), 6.68 (d, 2H, J = 8.7 Hz), 6.79 (d, 2H, J = 8.7 Hz), 7.82 (s, 1H). The pyrimidine-benzyl amine from the above reduction step was dissolved in CH_2Cl_2 (100 mL). There followed addition of Et_3N (500 μL, 660 mg, 6.52 mmol), and then at 0 °C dropwise addition of a solution of 20% phosgene in toluene (640 μL, 1.31 mmol). The mixture was stirred at 0 °C for 30 min, at room temperature for 1 h and then partitioned between EtOAc and water. The organic layer was dried over Na_2SO_4, filtered and concentrated and the residue was chromatographed on silica gel column with a 0–60% Et_2O in hexanes gradient to afford pyrimidopyrimidone **5** as a white foamy solid (543 mg, 89%; overall 57%). IR ($CHCl_3$) 3012, 2931, 2956, 2856, 1684, 1590, 1566, 1512, 1462, 1428, 1362, 1250 cm^{-1}. ^1H NMR (300 MHz, $CDCl_3$) δ 0.03 (s, 6H), 0.86 (s, 9H), 1.61 (m, 1H), 1.84 (m, 1H), 2.02–2.25 (m, 3H), 2.36 (ddd, 1H, J = 14.4, 9.0, 6.0 Hz), 2.54 (s, 3H), 3.78 (s, 3H), 4.49 (br m, 1H), 4.59 (dd, 2H, J = 14.1, 18.6 Hz), 5.56 (apparent p, 1H, J = 8.7 Hz), 6.91 (d, 2H, J = 8.7 Hz), 7.19 (d, 2H, J = 8.7 Hz), 8.05 (s, 1H). HRMS (ES+) for $C_{25}H_{36}N_4O_3SSi$ ($M+H^+$): Calcd 501.2350. Found 501.2353.

5.4. (±)-1-(*anti*-3-Hydroxy-cyclopentyl)-3-(4-methoxy-phenyl)-7-phenylamino-3,4-dihydro-1*H*-pyrimido[4,5-*d*]pyrimidin-2-one (6)

A solution of methylthio-pyrimidopyrimidine **5** (500 mg, 0.99 mmol) in THF (50 mL) was treated at room temperature with *m*CPBA 75% (483 mg, 2.10 mmol) for 2 h. The reaction mixture was then partitioned between EtOAc and aqueous saturated Na_2CO_3. The organic layer was dried over Na_2SO_4, filtered, concentrated and the residue was dissolved in aniline (5 mL). This

solution was then heated in a 100–110 °C oil bath for 9 h and then directly applied to a silica gel column. The column was eluted with a 0–30% Et_2O in toluene gradient to afford the intermediate O-TBS-protected analog of RO4383596 (420 mg, 77%). ^1H NMR (300 MHz, $CDCl_3$) δ 0.01 (s, 6H), 0.84 (s, 9H), 1.54 (br m, 1H), 1.83 (m, 1H), 2.08 (m, 3H), 2.39 (m, 1H), 3.77 (s, 3H), 4.44 (br m, 1H), 4.53 (s, 2H), 5.46 (apparent p, 1H, $J = 8.7$ Hz), 6.87 (d, 2H, $J = 8.7$ Hz), 7.03 (distorted t, 1H, $J = 7.5$ Hz), 7.17 (d, 2H, $J = 8.7$ Hz), 7.31 (apparent t, 2H, $J = 7.5$ Hz), 7.53 (d, 2H, $J = 7.5$ Hz), 7.91 (s, 1H). This O-TBS-protected analog was, without delay, dissolved at 0 °C in a 25% TFA in CH_2Cl_2 solution (10 mL) that also contained a small volume of H_2O (400 μL). After stirring for 30 min the reaction mixture was partitioned between EtOAc and aqueous saturated Na_2CO_3. The organic layer was dried over Na_2SO_4, concentrated and the residue was chromatographed on a silica gel column with a 0–100% EtOAc in hexanes to 0–30% THF in EtOAc gradient system. After a precipitation out of CH_2Cl_2 with excess of pentane RO4383596 was isolated as a white amorphous powder (309 mg, 95%; overall 73%). IR ($CHCl_3$) 3413, 2940, 1673, 1598, 1582, 1512, 1447, 1410, 1248 cm^{-1}. ^1H NMR (400 MHz, DMSO-d_6) δ 1.41 (br m, 1H), 1.67 (m, 1H), 1.93 (m, 3H), 2.23 (m, 1H), 3.66 (s, 3H), 4.20 (br s, 1H), 4.37 (d, 1H, $J = 3.3$ Hz), 4.50 (s, 2H), 5.38 (m, 1H), 6.85 (m, 3H), 7.17 (m, 4H), 7.62 (d, 2H, $J = 7.8$ Hz), 8.04 (s, 1H), 9.36 (s, 1H). HRMS (ES+) for $C_{24}H_{25}N_5O_3$ ($M+H^+$): Calcd 432.2030. Found 432.2036.

5.5. Kinase assays

KDR, FGFR, PDGFR, and EGFR kinase assays were conducted using homogeneous time resolved fluorescence (HTRF) assays. The KDR reactions contained 1 μM KDR substrate (Biotin-EEEEYFELVAKKKK), 1 nM activated KDR (recombinant human EE-tagged intracellular domain), dilutions of test compound (final reaction [DMSO] 1%) in kinase buffer (100 mM HEPES, pH 7.4, 1 mM DTT, 0.1 mM Na_2VO_4, 25 mM $MgCl_2$, 0.02% BSA, and ATP at the K_m of 0.3 mM). FGFR reactions contained 1.0 nM activated human recombinant GST-tagged intracellular domain (ICD), 1 μM substrate (Biotin-EEEEYFELV), test compound in 100 mM HEPES, 1 mM DTT, 0.4 mM $MgCl_2$, 0.4 mM $MnCl_2$, 50 mM NaCl, 1% DMSO, 10 μM ATP ($K_m = 8.5$ μM for FGFR), 0.1 mM Na_2VO_4, and 0.02% BSA. PDGFR and EGFR assays included human recombinant His-tagged ICD of PDGFR and recombinant human ICD of EGFR. For PDGFR and EGFR the substrate peptide used was Biotin-EEEEYFELV. ATP concentrations for these assays were at the K_m for each enzyme (2.3 μM for PDGFR and 0.5 μM for EGFR). CDK1/cyclin B, Erk2, AKT, PKCα, PKCδ, and Fyn assays were conducted using an assay based on immobilized metal assay for phosphochemicals (IMAP). This is a homogeneous FP-based technology (Molecular Devices) that enables quantitation of kinase activity via preferential binding of phosphorylated fluorescent peptide substrates to immobilized metal beads. Reactions were carried out at ATP concentrations of three times the K_m.

5.6. Endothelial cell proliferation assay

Human umbilical vein endothelial cells (HUVECs, Clonetics cat. #CC-2519) were cultured according to the manufacturer's protocol. Cell passages 2–6 were used to determine VEGF- or bFGF-stimulated proliferation. Subconfluent cultures were serum starved for 24 h, followed by the addition of test compound. After 2 h incubation with drug, 20 ng/mL VEGF (R&D Systems, cat. #293-VE) or 5 ng/mL bFGF (purified, recombinant) were added. DNA synthesis was evaluated using BrdU incorporation (Roche Biochemicals, cat. #1-647-229). After 20 h of incubation with compound, BrdU labeling reagent was added. Four hours later, incorporated label was quantitated using a peroxidase-conjugated BrdU antibody and colorimetric detection.

5.7. Tumor cell tetrazolium dye proliferation assay

Exponentially growing tumor cells were plated in 96-well microtitre plates and incubated overnight at 37 °C prior to compound addition. Proliferation was assessed by measurement of formazan formation from 3-(4,5-dimethylthiazole-2-yl)-2,5-diphenyl-2*H*-tetrazolium bromide (MTT) (Sigma) during a 2.5 h incubation 6 days after initial plating.

5.8. Immunoblotting

HUVECs (Clonetics cat. #CC-2519), passages 2–4 were grown according to the manufacturer's protocol to 70% confluency, were serum starved (EBM-2 plus 1.0% HI-FBS) for 18 h. Test compound was added 1 h prior to VEGF stimulation (50 ng/mL rhVEGF, R&D Systems cat. #293-VE). Cells were washed and lysed (in modified RIPA buffer) on ice for 5 min after addition of growth factor. Lysates were subjected to centrifugation (14,000*g*) and pellets were discarded. Protein concentration was determined using the Bio-Rad protein assay reagent. Twenty milligrams of total soluble protein was loaded per lane onto Novex 4–20% gradient gels, proteins were resolved by electrophoresis (according to Novex protocol), transferred to nitrocellulose membranes, immunoblotted, and specific binding detected using ECL. Antibodies, vendors are as follows: rabbit anti-PhosphoKDR Receptor 2 (Cell Signaling, cat. #2474); Mouse anti-KDR (IC) IgG (Upstate Biotechnology, Inc., cat. #05-554); rabbit anti-phosphoErk1/2 (Cell Signaling, cat. #9101); rabbit anti-phosphoAKT (Ser473) (Cell Signaling, cat. #9271); rabbit anti-AKT (Cell Signaling, cat. #9272); rabbit anti-Erk1/2 (Upstate Biotechnology, Inc., cat. #06182); mouse anti-β actin (Sigma, cat. #A-5316); HRP: goat anti-rabbit IgG (Cell Signaling cat. #7074); and HRP-goat anti-mouse IgG (Cell Signaling cat. #7076). Actin controls (not shown) were used to normalize protein loading.

5.9. Corneal pocket assay

The test compound was evaluated for anti-angiogenic activity in bFGF- and VEGF-driven corneal neovascularization assays in female C57/BL6 mice (5–7 weeks old). Pellets impregnated with bFGF or VEGF were implanted and treatment was initiated the same day. In the bFGF assay, animals were dosed orally for 5 days. In the VEGF assay animals were dosed for 7 days prior to quantitation of the area of vascularization. All animals were dosed twice a day for the duration of the experiment.

5.10. C57/BL6 chronic-dose pharmacokinetics

Test compound was administrated orally twice a day for 5 days, to C57/BL6 mice at a dose level of 25, 50, and 100 mg/kg. The test compound used in this investigation was provided in suspension in 2% Klucel LF and 0.1% Tween 80 in water. Constant dosing volumes of 0.2 mL per dose were used. In each dose group, six mice were divided into two subgroups throughout the experiment. The same subgroup of three animals was used for every other time point. Blood samples were collected via retro-orbital bleed at 0, 1, 4, and 8 h post-dose. Collection tubes contained EDTA as anticoagulant. After centrifugation, plasma was removed and stored frozen at −70 °C until analysis.

5.11. Athymic nude mouse single-dose pharmacokinetics

A single dose of test compound was administered to athymic nude mice intravenously at a dose level of 10 mg/kg, or orally at a dose level of 50 mg/kg. The test compound used for intravenous administration was formulated in 2% DMA, 10% PEG400, and 88% of 40% HPBCD in water, while the oral formulation was in 2% Klucel LF and 0.1% Tween 80 in water. The dosing volume used was 0.2 mL for both iv and oral dosing. Blood samples were collected from the retro-orbital sinus or via terminal cardiac puncture at 1, 5, 15, and 30 min, and 1, 2, 4, 8, 16, and 24 h post-dose after iv dosing and 5, 15, and 30 min, and 1, 2, 4, 8, 16, and 24 h post-dose after oral dosing. Collection tubes contained EDTA as anticoagulant. After centrifugation, plasma was removed and stored frozen at −70 °C until analysis.

5.12. Wistar rat single-dose pharmacokinetics

A 5 mg/kg single dose of test compound was administered to Wistar rats intravenously via a femoral arterial catheter. Compound was also dosed orally at 50 mg/kg. The test compound used for intravenous administration was formulated in 2% DMA, 10% PEG400, and 88% of 40% HPBCD in water, while the oral formulation was 2% Klucel LF and 0.1% Tween 80 in water. The dosing volume was at 5 mL/kg orally and 2.5 mL/kg iv. Blood samples were collected via an implanted jugular catheter at 1, 7, 15, and 30 min, and 1, 3, 6, 12 and 24 h post-dose after iv dosing and 5, 15, and 30 min, and 1, 3, 6, 12, 24 and 48 h post-dose after oral dosing. Collection tubes contained EDTA as anticoagulant. After centrifugation, plasma was removed and stored frozen at −70 °C until analysis.

5.13. Analytical method for measurement of levels of test compound in rodent plasma

A specific LC-MS/MS assay was used for this study to detect the test compound in plasma samples from mice and rats. Fifty microliters of samples was extracted by precipitation of plasma proteins with acetonitrile. The supernatant was diluted with water before injecting onto a C18 (Zorbax® SB-C18 5 μm 2.1 × 50 mm) LC column connected to an LC/MS/MS system. Standard and QC samples were injected together with study samples. Results of back-calculated standards and QC samples met our non-GLP acceptance criteria. All concentrations were interpolated from calibration curves, which ranged from 1 to 2000 ng/mL using an internally validated Watson laboratory information system (LIMS) software program (version 6.3.0.01a).

5.14. Single- and chronic-dose pharmacokinetic analysis

All pharmacokinetic (PK) parameters were calculated using Watson LIMS (v 6.3.0.01a). For each dose group of mice, the mean plasma concentrations for each time point were obtained for three mice. The chronic-dose PK parameters were estimated from the mean plasma concentration data. Sampling times are reported as nominal time. The limit of detection was 1–1000 ng/mL and samples with concentrations reported below the level of quantitation were disregarded. Parameters reported are the maximum plasma concentration (C_{max}), time to reach the maximum plasma concentration T_{max}, and area under the plasma concentration–time curve from 0 to the last sampling time point (AUC_{0-8h}). The observed C_{max} and T_{max} were taken directly from the mean plasma concentration–time profiles. AUC was calculated using the linear trapezoidal rule. In addition, PK parameters were estimated in mice and rats. Composite PK parameters were estimated for mice, while individual PK parameters were estimated for rat and averaged to report the means. Clearance (Cl) and volume of distribution at steady state (V_{dss}), and half-life ($t_{1/2}$) were estimated by non-compartmental analysis. $AUC_{0-\infty}$ was calculated by non-compartmental analysis and extrapolated to infinity using the apparent elimination rate constant λz, with extrapolation from the calculated concentration at the last time point. Oral bioavailability was estimated as a ratio of dose-normalized oral AUC to iv AUC.

Acknowledgments

We are grateful to Gino Sasso, Richard Szypula, Vance Bell and Theresa Burchfield for their analytical and spectroscopic work.

References and notes

1. (a) For reviews on the signaling cascades and processes involved in angiogenesis, see: Griffioen, A. W.; Molema, G. *Pharmacol. Rev.* **2000**, *52*, 237; (b) Yancopoulos, G. D.; Davis, S.; Gale, N. W.; Rudge, J. S.; Wiengand, S. J.;

Holash, J. *Nature* **2000**, *407*, 242; (c) Bikfalvi, A.; Bicknell, R. *Trends Pharmacol. Sci.* **2002**, *23*, 576; (d) Bicknell, R.; Harris, A. *Annu. Rev. Pharmacol. Toxicol.* **2004**, *44*, 219.
2. For a overview of the clinical aspects of anti-angiogenic therapies, see: Bergers, G.; Benjamin, L. E. *Nat. Rev.* **2003**, *2*, 401.
3. (a) Folkman, J. *N. Engl. J. Med.* **1971**, *285*, 1182; (b) Folkman, J. *Sci. Am.* **1976**, *234*, 58.
4. (a) www.cancer.gov/clinicaltrials/developments/anti-angio-table; (b) www.clinicaltrials.gov; search term: anti-angiogenesis.
5. Two such small and orally bioavailable molecules, erlotinib (Tarceva®) and gefitinib (Iressa®), were recently approved by the US FDA for the treatment of non-small-cell lung cancer (NSCLC). Both molecules are selective inhibitors of the pro-angiogenic tyrosine kinase EGFR
6. (a) For some reviews on small molecule inhibitors of pro-angiogenic RTKs, see: Mazitscheck, R.; Giannis, A. *Curr. Opin. Chem. Biol.* **2004**, *8*, 432; (b) Traxler, P. *Exp. Opin. Ther. Targets* **2003**, *7*, 215; (c) Magnetti, F.; Botta, M. *Curr. Pharm. Des.* **2003**, *9*, 567; (d) Boyer, S. J. *Curr. Top. Med. Chem.* **2002**, *2*, 973.
7. (a) Shaheen, R. M.; Tseng, W. W.; Davis, D. W.; Liu, W.; Reinmuth, N.; Vellagas, R.; Wieczoreck, A. A.; Ogura, Y.; McConkey, D. J.; Drazan, K. E.; Bucana, C. D.; McMahon, G.; Ellis, L. M. *Cancer Res.* **2001**, *61*, 1464; (b) Bergers, G.; Song, S.; Myer-Morse, N.; Bergsland, E.; Hanahan, D. *J. Clin. Invest.* **2003**, *111*, 1287; (c) Erber, R.; Thurnher, A.; Katsen, A. D.; Groth, G.; Kerger, H.; Hammes, H. P.; Menger, M. D.; Ullrich, A.; Vajkoczy, P. *FASEB J.* **2004**, *18*, 338.
8. Rossman, P.; Luk, K.; Cai, J.; Chen, Y.; Daniewski, A. R.; Dermatakis, A.; Flynn, T.; Garofalo, L.; Gillespie, P.; Goodnow, R.; Graves, B.; Harris, W.; Huby, N.; Jackson, N.; Kabat, M.; Konzelmann, F.; Li, S.; Liu, J.-J.; Liu, W.; Lukacs, C.; Michoud, C.; Perrotta, L.; Portland, L.; Qiao, J.; Roberts, J.; Schutt, A.; Simcox, M.; So, S.-S.; Tamborini, B.; Toth, K.; Wen, Y.; Xiang, Q.; Yang H.; Zhang, Z. In *Proc. Am. Accos. Cancer Res. Orlando, FL, U.S.A.* **2004**, *45*, Abst. 2478.
9. Dermatakis, A.; Luk, K.-C.; DePinto, W. *Bioorg. Med. Chem.* **2003**, *11*, 1873.
10. Both enantiomers of RO4383596 were also synthesized and found to have similar potencies and selectivities as the racemic RO4383596. For instance, the (+)-(*R*,*R*)-enantiomer had an IC_{50} of 12 nM against KDR, 35 nM against FGFR, 239 nM against EGFR and 28 nM against PDGFR. The IC_{50}s for the (−)-(*S*,*S*)-enantiomer were: 15 nM against KDR, 37 nM against FGFR, 365 nM against EGFR, and 33 nM against PGDFR, respectively.
11. A single 100 mg/kg oral dose of RO4383596 was also administered to a separate group of B57/C6 female mice. The median pharmacokinetic parameters calculated for that cohort of mice were: AUC = 145,806 ng h/mL; AUC/dose = 1458 ng h/mL/mg/kg; C_{max} = 37,600 ng/mL and T_{max} = 0.5 h. The above data show no appreciable difference from the data obtained with the group of mice that were treated chronically (twice a day for 5 days) with 100 mg/kg of RO4383596 (Table 5). This suggests that the observed pharmacokinetic parameters and efficacy of RO4383596 upon chronic dosing were not because of drug accumulation.
12. For a compilation of the in vivo, and in vitro, assays currently in use for the assessment of the angiogenic potential of inducers and inhibitors, see: Auerbach, R.; Lewis, R.; Shinners, B.; Kubai, L.; Akhtar, N. *Clin. Chem.* **2003**, *49*, 32.